Computer Simulation Approach to the Chemical Mechanisms of Self-Propagating High-Temperature Reactions: Effect of Phase Transitions on the Thermite Reaction between O_2 Gas and Zr Powders

Filippo Maglia,* Umberto Anselmi-Tamburini, Silvia Gennari, and Giorgio Spinolo

INSTM, CSTE/CNR, and Department Physical Chemistry, University of Pavia, Viale Taramelli, 16, I 27100 Pavia, Italy

Received: January 9, 2002

The $Zr + O_2 \rightarrow ZrO_2$ self-propagating high-temperature synthesis (SHS) has been investigated by computer simulation with a model accounting for two concurrent oxidation mechanisms (solid-state diffusion and gas-phase transport of oxygen) and for melting of reagent and product, under the external conditions defined by two process parameters: amount of zirconia added as diluent in the starting mixture (dilution degree) and partial pressure of oxygen reagent. The results are compared with those of a closely similar model that does not account for the phase transitions. Allowance for phase transitions shows many marked effects on the dynamic behavior of the SHS (which propagates in a steady mode under a wider range of dilution degrees) and on the macrokinetic parameters (space and time profiles of temperature and advancement degree of oxidation and time evolutions of wave speed and combustion temperature). These effects can be used for assessing the mechanism of an SHS from real experiments.

1. Introduction

Self-propagating high-temperature synthesis (SHS) is now a popular and well-established synthetic technique.[1−7] The method essentially requires an heterogeneous and sufficiently exothermic chemical reaction involving at least one solid reactant. After ignition by a suitable external energy pulse, a reaction front is formed and propagates through the heterogeneous mixture of the reactants in form of a steady thermal and chemical wave.

While most of the scientific interest toward SHS is due to technological reasons, such as its wide range feasibility, simplicity and low cost of the apparatus, and excellent properties of the materials so obtained, SHS has also attracted attention from the theoretical point of view as a model system for investigating the dynamic features of the coupling between a (thermally activated) chemical reaction and energy and mass transport.

Analytic and numerical studies[8−12] have indeed shown a complex behavior associated with propagation and extinction of the combustion. A deeply investigated feature is the evolution with increasing heat loss of the steady combustion (which propagates with constant velocity and shape) into several unsteady modes, and finally into extinction. The route to extinction first includes a simple oscillatory combustion, that is a combustion mode exhibiting velocity and composition and temperature profiles which change periodically with time and space. With increasing heat loss, further Hopf bifurcations may occur, with transitions to more complex periodic modes, and eventually to chaotic behavior. The sequence of the unsteady propagation modes actually depends on the investigated model, in particular on the allowance for melting of the solid reactant.

In these approaches, an SHS reaction is typically considered as very similar to a gas-phase combustion and a unified treatment as a function of the Lewis (Le) number is sometimes discussed. Concerning the assumed mechanisms, the similarity with gas-phase reactions is based on the assumption of a gas-phase first-order kinetic law. A general lack of consistency between experimental and theoretical work has been noted,[13−15] and has been ascribed to the intrinsic deficiencies of the theoretical treatments based on the similarity with homogeneous flame theory. Indeed, an SHS can involve many different processes, such as gas/solid, solid/liquid or solid/solid reactions, with gas-phase homogeneous reactions playing a minor role (if any). Modeling each of these processes with the concentration-power laws of gas-phase reactions cannot account, for instance, for the marked particle-size effects typically shown by an SHS. Also, it does not seem reasonable to assume that a single mechanism is rate determining over the extremely wide ranges of temperatures, thermal gradients, and chemical potentials experienced by a real SHS.

As a matter of fact, the experimental investigation of the chemical mechanisms of SHS reactions is presently characterized by a noteworthy lack of powerful methods. The direct investigation of the process is usually limited to some global macrokinetic determinations such as the time and space profiles of temperature, and the time evolution of combustion temperature (i.e., the maximum temperature along a space profile) or speed of the thermal wave. Only indirect mechanistic insights are provided by phase and composition analysis and by microscopic observation of the samples at the end of the process, or after a thermal quenching. In this respect, computer simulation is important not only for investigating existence and features of the various propagation modes, but also as a direct support to the experimental investigation of the reaction mechanisms. Numerical simulations based on assumed mechanisms can be compared with experiments for assessing or discarding these mechanisms, and for suggesting further experiments. According to this line of thinking, a computer simulation does not need to

* Corresponding author: Department of Physical Chemistry, University of Pavia, Viale Taramelli, 16, 27100 Pavia, Italy. Fax: +39 0382 507575. E-mail: filippo@chifis.unipv.it.

10.1021/jp020028s CCC: $22.00
Published on Web 05/18/2002

reproduce exactly the experimental data. Such a refined computation may typically require parameters of kinetic nature that are not previously known, that can be determined only after a trustworthy assessment of the mechanism, or else that are impossible to determine independently of an SHS experiment. What is really required is a tool for exploring the effect of the real process variables: that is, determining the trend of the scarce experimentally measurable quantities as a function of the variables that is actually possible to change from experiment to experiment on the same chemical system.

A flexible simulation method for investigating, with this particular aim, the chemical mechanisms of SHS processes has been presented in previous papers.[13,14] The method was applied to the SHS between Zr and O_2 (in the presence of ZrO_2 diluent) to produce ZrO_2 using a one-dimensional model which takes into account two concurrent oxidation mechanisms (solid state diffusion of oxygen in the oxide layer which grows on the metal particle, and sticking of oxygen gas onto the reacting particle) but does not take into account permeation of the reactant gas into the heterogeneous assembly of grains of the reacting pellet and the phase transitions of solid reactant or product. The computer simulations have been made by considering different quantities of ZrO_2 diluent, different sizes of the reacting zirconium particles, and different pressures of the oxygen environment, as these are the process variables of a real SHS experiment. Concerning the dynamic behavior, a noteworthy feature of this model is that the concurrent mechanisms respectively show positive and negative feedback.

The numerical results obtained are in nice qualitative agreement with the previously cited results with gas-phase kinetics.[8−12] For instance, the $Zr + O_2 \rightarrow ZrO_2$ SHS shows (in addition to steady combustion) a pulsating combustion regime, that is a simple oscillatory propagation mode where the wave front parameters (wave velocity and combustion temperature) are periodic in time. The space profiles of temperature and composition variables also change periodically with time and after a constant time interval show again the same shape (examples of the steady and simple pulsating propagation modes are reported on Figure 1). Using progressively 'colder' reaction conditions (which is realized by considering a larger amount of inert diluent), a more complex periodic propagation appears, where the time evolution of wave velocity and combustion temperature is characterized by two periodic minima and maxima, and eventually the SHS turns into a chaotic behavior just before extinction. All these features are conveniently summarized by a phase diagram, such as that of Figure 2, where the domains pertinent to the various propagation modes are drawn in the space of the investigated process variables.

The computer simulations have shown that the two underlying mechanisms are made well apparent by different trends of the macrokinetic parameters (combustion temperature and wave speed) of the SHS with respect to the process variables. For instance, when solid state diffusion is the rate limiting process, the macrokinetic parameters show a well clear linear dependence on the reciprocal particle size, which drops down at low oxygen pressure, where the nature of the rate limiting process changes. Wave speed and combustion temperature are correspondingly independent or dependent on oxygen pressure at fixed particle size. Concerning the dilution degree, the macrokinetic parameters generally decrease with increasing dilution and the onset of rate control by oxygen pressure is most typically characterized by an enlargement of the dilution range where the propagation mode is stationary.

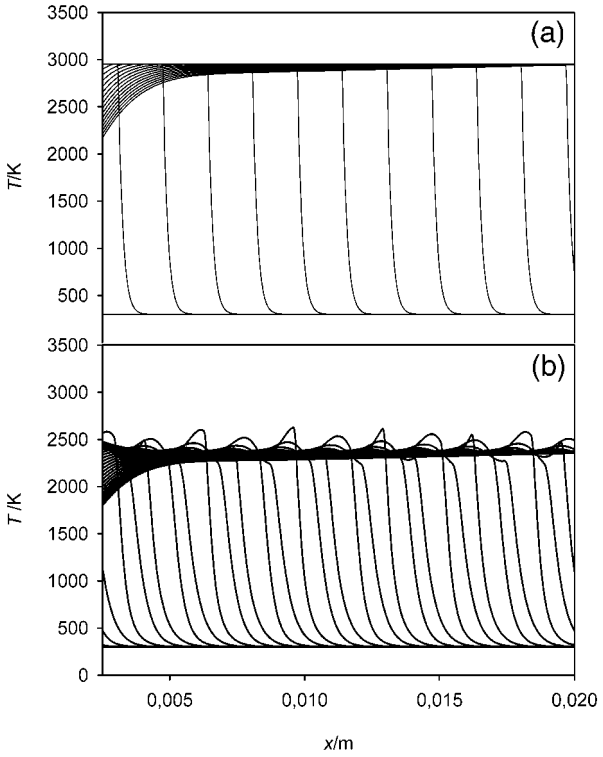

Figure 1. Temperature at different times as a function of position along the sample under $P(O_2) = 1$ atm in case of steady (plot a, $D = 0.80$) and pulsating (plot b, $D = 0.85$) propagation. Both profiles are sampled at constant time intervals. A larger interval is used in part b.

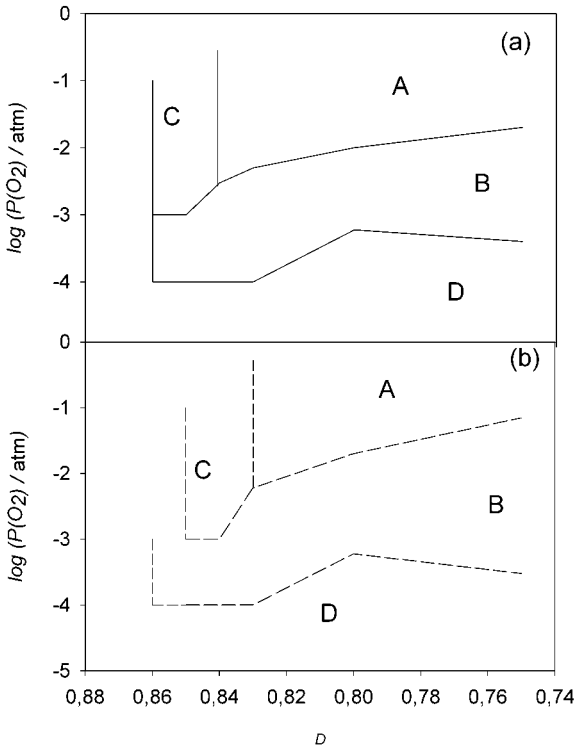

Figure 2. Mode diagram for the combustion process as a function of D and $P(O_2)$ with (solid line) and without (dashed line) phase transitions. Region A: steady combustion under diffusion control; region B: steady combustion under pressure control. Region C: oscillatory (unsteady) combustion modes (under diffusion control). Region D: the SHS does not self-propagate.

Aim of the present work is to go beyond what we believe is the most significant restriction of the kinetic model investigated so far, and to explore the role played by the phase transitions

of reactant (Zr) and product (ZrO_2) on the self-propagating Zr + O_2 system. A comparison between the reaction characteristics with and without taking into account melting of reactants and products has been performed by considering the following aspects: (a) the dependence of wave speed and combustion temperature on the degree of dilution and oxygen partial pressure, (b) the transition between the diffusion controlled and the pressure controlled mechanism, (c) dependence of the extinction limit from oxygen partial pressure, and (d) the transition from steady to simple or complex pulsed propagation and to extinction as a function of degree of dilution at the pressure regimes where diffusion and pressure control, respectively, are active.

2. Computational Details

Detailed presentation and guidelines of the computational method have been reported previously.[13,14] We give here only a short summary with emphasis on numerical data, improvements, or changes.

The computational method is based on the uncoupling between micro- and macrokinetics. The microkinetic treatment takes care of the chemistry, which can be divided at will into different steps (phase transformations and chemical reactions) with several kinetic laws (mechanisms) for each step. All these laws describe the behavior of the system at the level of the grains of the solid reactant(s). The steps now considered are (a) oxidation, (b) melting of the zirconium reactant, and (c) melting of zirconia (product or diluent). For the first step, two concurrent mechanisms are assumed as before:[13,14] the diffusion-controlled growth of an oxide layer on a metal particle with initial radius r_0, and the flux of molecular oxygen sticking on the external surface of the partially reacted particle. The melting steps are modeled in the simplest manner as entirely controlled by heat flow without explicit kinetic law.

At the macro-kinetic level, the conversion degrees of the various steps are inserted into the Fourier heat balance equation, which is solved by a Crank−Nicholson FD (finite differences) algorithm. At each time step, after upgrade of temperature by the FD routine (and before upgrade of the advancement degree of the oxidation step) the advancement degrees of the two melting steps are updated on the basis of heat balance alone, if a component crosses its equilibrium transition temperature.

The enthalpies of the components (Zr, ZrO_2, and O_2) are modeled with simple linear dependence on temperature, that is with temperature independent heat capacities, which has been obtained by a kind of smoothing of the available thermal data.[16] The thermodynamic data used in the simulation (see Figure 3) are

$$H_{Zr(s)} = -11133.62 + 33.969T \qquad T < 2125\ \text{K}$$

$$H_{Zr(l)} = -9162.96 + 33.472T \qquad T > 2125\ \text{K}$$

$$H_{ZrO_2(s)} = -1127322.68 + 78.08T \qquad T < 2950\ \text{K}$$

$$H_{ZrO_2(l)} = -1031395.68 + 74.47T \qquad T > 2950\ \text{K}$$

$$H_{O_2(g)} = -12718.35 + 36.35T$$

(in the whole temperature range)

When phase transitions are not taken into account, the linear dependence for both solid Zr and ZrO_2 is used in the whole temperature range. It should be noted that these data are slightly different from those of the previous simulations,[13] where a less simplified temperature dependence was used. For that reason, the simulations 'without phase transitions' have been remade to allow a better comparison.

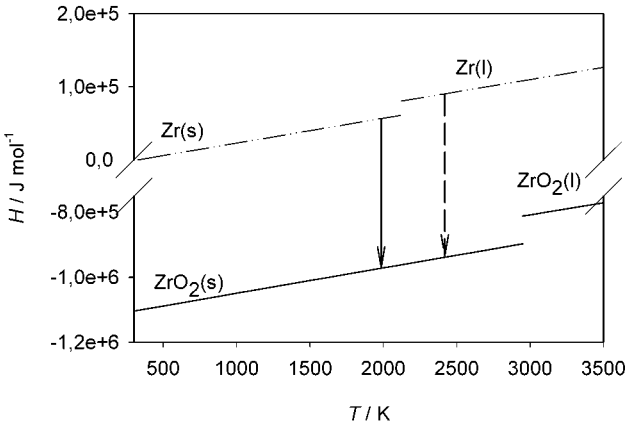

Figure 3. Molar enthalpy of solid reagent and product as a function of temperature. The arrows refer to the reaction of solid (solid arrow) or liquid (dashed arrow) reactant producing solid ZrO_2.

The adiabatic temperature of the SHS process depends on the amount of solid diluent (ZrO_2) in the starting mixture, which is one of the investigated process parameters. For a significant range of starting compositions, this amount actually corresponds to a final state where solid and liquid ZrO_2 coexist, so that the adiabatic SHS temperature is fixed at the melting point of ZrO_2. This point will be discussed later in some detail. Meanwhile, we note that for this reason the comparison between the simulations "with" and "without" phase transitions can be somewhat misleading and must be done with some attention.

Density and thermal conductivity data are taken from literature,[16] while a simple additive law for thermal conductivity of heterogeneous materials was assumed. The external diameter of the cylindrical sample was fixed at 10 mm (this quantity determines the radiation heat loss toward the surrounding atmosphere kept at room temperature).

3. Results and Discussion

The process variables investigated in the present work are (a) oxygen partial pressure and (b) degree of dilution (D) defined as

$$D = \frac{n(\text{ZrO}_2\ \text{dil})}{n(\text{Zr}) + n(\text{ZrO}_2\ \text{dil})}$$

where n is the *starting* molar quantity of the corresponding substance.

The process variables have been varied between 10^2 and 10^{-5} atm and between 0.5 and 0.9, respectively. These ranges correspond to the typical conditions of a real SHS experiment[17,18] (the SHS between Zr and oxygen gas is highly exothermic, and some degree of dilution is unavoidable) and cover the whole set of combustion regimes. In all simulation runs, the third process variable (the initial size of the reacting zirconium particles, r_0) has been kept fixed at 10 μm.

3.1. Steady Propagation. At sufficiently low dilution degrees, when the reaction is highly exothermic, the propagation of the combustion wave is characterized by unique values of velocity and temperature (steady combustion mode). As already said, within the range of dilution corresponding to stationary propagation the reaction rate can be controlled by oxygen anion diffusion in the solid oxide layer (a situation referred to as diffusion control in the followings) or by sticking of the oxygen

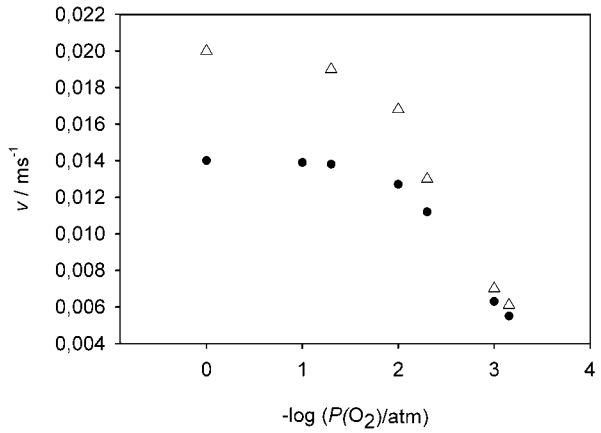

Figure 4. Wave velocity (v) as a function of $P(O_2)$ at $D = 0.75$ with (full circles) and without (empty triangles) phase transitions.

gas molecules onto the external surface of the reacting grain (a situation referred to as pressure control), depending on the oxygen partial pressure.

The influence of the phase transitions on the stationary combustion mode and the underlying mechanisms can be best visualized by considering the evolution of the reaction parameters (velocity, temperature, advancement degrees, ...) as a function of the oxygen partial pressure at $D < 0.81$. Figure 4 shows the dependence of the wave velocity on $P(O_2)$ for the models with and without phase transitions at $D = 0.75$. At high oxygen pressure the wave velocities are independent of pressure, but the asymptotic values are considerably different for the two models: 0.020 and 0.014 cm s^{-1}, respectively. On the contrary, at low oxygen pressures, the macrokinetic parameter becomes heavily pressure dependent, but the difference between the two models disappears.

A more detailed description of these trends can be obtained by considering the space profiles (at fixed time) of the variables of the PDE Fourier system (temperature and the advancement degrees of the chemical steps). These are shown on Figures 5 and 6, where the rate of the oxidation reaction ($\partial\,\eta/\partial\,t$) is plotted instead of the advancement degree (η) for better clarity. As described in the previous works, a bell shaped ($\partial\eta/\partial t$) plot is indicative of a full control by solid-state diffusion, while a truncated shape is due to the onset of (partial) pressure control.

Figure 5 shows that diffusion control holds for both models at high pressure. The rates ($\partial\eta/\partial t$) are plotted on the same (arbitrary) scale and it is apparent that the reaction proceeds more rapidly in absence of phase transitions, since the space integral of the reaction rate measures the wave speed. The effect of phase transitions can be clearly outlined also observing the temperature profiles. In part a, the temperature profile does not exceed ZrO_2 melting point, because the reaction enthalpy is not sufficient to melt the product completely, while in part b a much higher temperature is reached. This is a general feature of the investigated system: when phase transitions are considered the temperature cannot exceed the ZrO_2 melting point (unless D values so low to be meaningless from a practical point of view are selected). This is the cause of the significantly lower wave speed experienced by the model with phase transition under diffusion control (Figure 4), and of the previous observation that, when lower pressures are considered and the combustion temperature decreases below the melting point of zirconia, the difference between the two models disappears.

In Figure 5a, a knee corresponding to Zr melting point (2125 K) can also be observed on the raising portion of the temperature profile. The third plot of the same figure corresponds to the

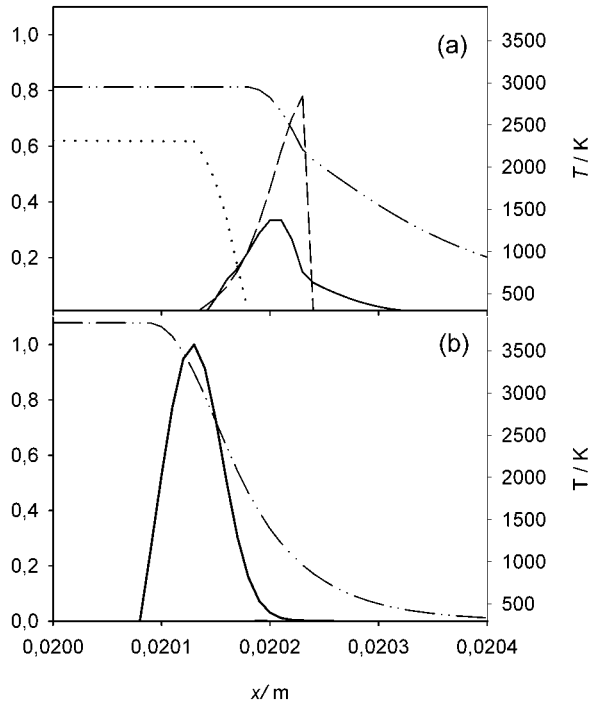

Figure 5. Temperature (dash−dot line, right axis), reaction rate (continuous line), fraction of molten product (dotted line, left axis) and fraction of molten metal (dashed line, left axis) as a function of position within the sample at fixed time with (plot a) and without (plot b) phase transitions for $D = 0.75$ and $P(O_2) = 1$ atm. The reaction is under solid-state diffusion control. The reaction rates are plotted on the same arbitrary scale.

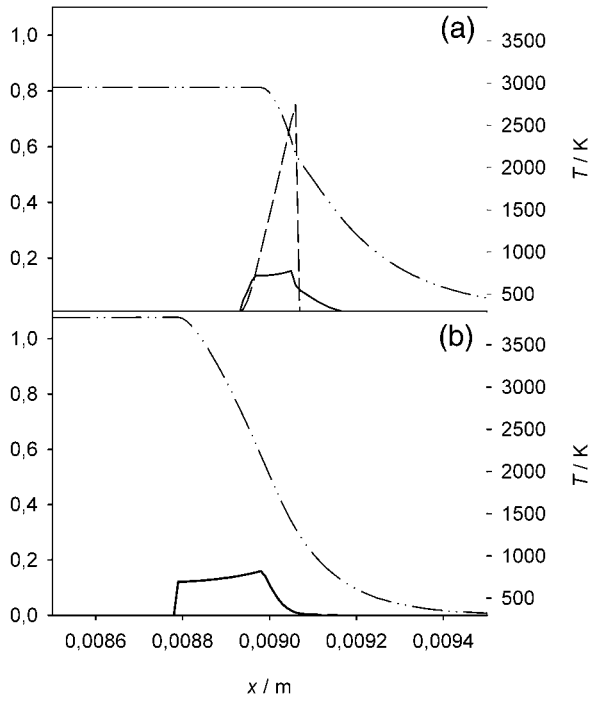

Figure 6. Temperature (dash−dot line, right axis), reaction rate (continuous line) and fraction of molten metal (dashed line, left axis) as a function of position within the sample at fixed time with (plot a) and without (plot b) phase transitions for the SHS at $D = 0.75$ and $P(O_2) = 10^{-3}$ atm. The reaction is under gas pressure control. The reaction rates are plotted on the same arbitrary scale.

amount of liquid zirconium. By comparing this plot with the bell shaped plot of oxidation rate ($\partial\eta/\partial t$), one can see how most of the zirconium reacts in the liquid state while only a small fraction reacts as a solid; a sharp increase in the ($\partial\eta/\partial t$) plot

can also be observed as temperature reaches the Zr melting point. On the other hand, oxide melting occurs as the reaction has almost reached its completion.

As $P(O_2)$ is lowered below 10^{-3} atm, the reaction turns to pressure control (Figure 6). While Figure 4 shows that the onset of the pressure control occurs at lower pressure in the presence of phase transitions, Figure 6 indicates more precisely that this is due to the lower value of the diffusion controlled reaction rate when phase transitions are considered. In other words, (a) the diffusion controlled reaction rates are different from each other, but are both pressure independent; (b) the pressure controlled reaction rates are practically independent of the presence of phase transitions (this is due to the inverse square root dependence of rate from temperature in the underlying models, and can be clearly seen by comparing parts a and b of Figure 6); therefore, (c) the pressure controlled rate becomes determining (lower than the diffusion controlled rate) at a lower pressure for the model with phase transition. Part a of Figure 6 also shows that speaking of pressure control is somewhat inappropriate, since the oxygen sticking mechanism actually holds when the reaction is around its maximum rate: some amount of diffusion control still holds in the initial and final stages of the reaction, but becomes progressively less important as oxygen pressure decreases. Figure 6 also shows that, similarly to what observed at higher pressures (Figure 5), most of the Zr oxidation occurs in the molten state.

It is also worth noting that, according to Figure 4, steady combustion directly turns into extinction, without unsteady propagation modes, and that extinction occurs at an identical pressure for both models considered. Such an equality is not restricted to a particular composition range but is valid at any D value.

3.2. Oscillatory Propagation. The above picture holds for a wide range of D values until the propagation mode changes from steady propagation (Figure 1a) to oscillatory propagation (Figure 1b) due to the lower exothermicity.

Figure 7 shows the dependence of wave speed and combustion temperature on D under $P(O_2) = 1$ atm for the two models with and without phase transition. As long as stationary propagation is active ($D < 0.82$), a similar decrease with increasing dilution can be observed in the absence of phase transitions for both combustion temperature and wave velocity. As expected, the wave velocity decreases also when phase transitions are considered, while temperature is limited by melting of the oxide to 2950 K and therefore starts to decrease after a threshold D value is reached. Analogously to what observed in the previous paragraph, combustion temperature and wave speed values are considerably higher when phase transitions are not taken into account and the difference between the two models decreases with increasing D.

As D approaches the limit for extinction, instabilities in the front propagation were found. The SHS propagates with well defined oscillations of both combustion temperature and wave velocity and with time dependent space profiles of temperature and of the composition variables (Figure 1b). After a more or less prolonged initial ignition transient, wave speed and combustion temperature oscillations are constant in both amplitude and frequency. The occurrence of the oscillatory modes is markedly influenced by the model employed. The melting of reactants and products plays in fact an important role in damping the oscillatory behavior. The damping effect can be visualized in two different ways: (a) the onset of the oscillations occurs at higher D and (b) the amplitude of the oscillations is, at any D, less pronounced when melting is taken into account. Figure 7 indicates at $D = 0.83$ and $D = 0.82$ the boundary between the steady and unsteady modes respectively with and without transitions. To make apparent these effects, two values of velocity and combustion temperature (both the maximum and the minimum) are shown.

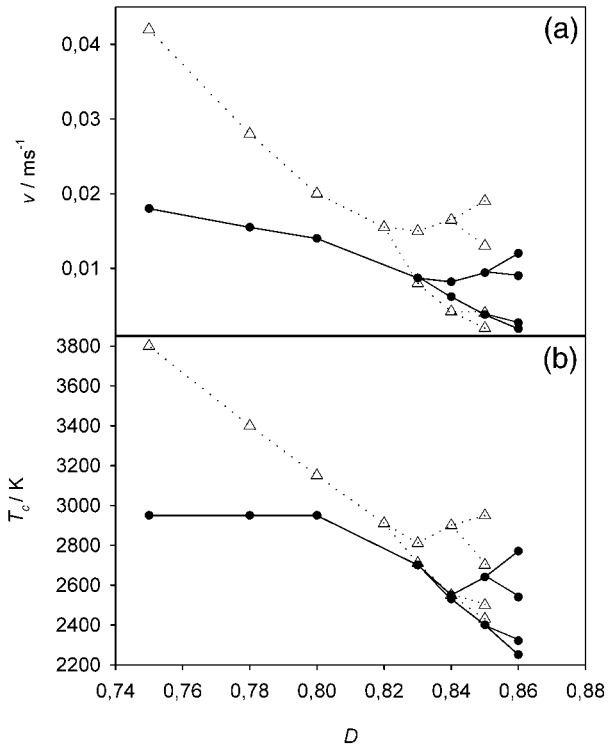

Figure 7. Wave velocity (v, plot a) and combustion temperature (T_c, plot b) as a function of D at $P(O_2) = 1$ atm with (full circles) and without (empty triangles) phase transitions. Where two values at the same D are shown, the SHS propagates with a simple pulsating mode (see also Figure 9); where four values are shown, the SHS propagates as described by Figure 10.

It must be remarked as phase transitions play a damping effect also when the propagation is stationary, in the initial stage of the reaction, by shortening the initial transient, during which oscillations are generally present due to the ignition process (Figure 8).

The unsteady propagation so far described is a simple pulsating one. As dilution is further increased, a transition to more complex oscillatory modes is observed in both models. Combustion temperature and velocity now show a double oscillation with a relative minimum and maximum in addition to the absolute ones (Figure 7). To make clear the further bifurcation, Figure 7 shows in this case the value corresponding to both absolute and relative minima and maxima. From the figure, it is apparent that also the onset of this more complex mode occurs at a higher D when phase transformations are considered. Even more important, the presence of phase transitions extends the range of existence of the whole set of combustive modes to higher degree of dilution (up to $D = 0.86$, instead of $D = 0.85$).

Interesting insights on the effect of phase transitions on the reaction behavior in the unsteady regimes can be obtained by the inspection of Figures 9 and 10. Figure 9 shows the trend of wave velocity as function of time (part a) and the trends of temperature, oxidation rate ($\partial\eta/\partial t$) and amount of molten Zr as a function of space at given times for a simple oscillatory behavior (parts b and c). Parts b and c refer to a time when the combustion temperature reaches a maximum or minimum,

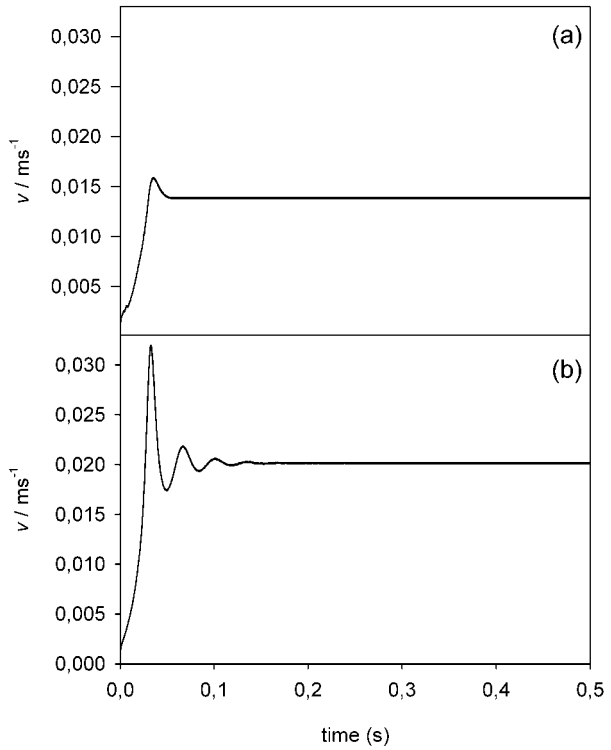

Figure 8. Wave velocity as a function of time at $P(O_2) = 1$ atm and $D = 0.80$ with (plot a) and without (plot b) phase transitions. The constant value corresponds to attainment of steady combustion.

respectively. The reaction rate ($\partial\eta/\partial t$) plots clearly indicate as the reaction front is much sharper in correspondence to the oscillation maximum; also zirconium melting occurs much earlier at the reaction maximum while at the minimum approximately half of it is oxidized in the solid state. In both cases, as already observed before, Zr melting accelerates the reaction. It is finally interesting to underline that, in correspondence to the maximum, not only the temperature peak value is higher, but there is also a more pronounced preheating of the region ahead of the reaction front as evident from the sharper temperature profile.

Figure 10 illustrates the situation in correspondence to two maxima (an absolute maximum (part b) and a relative one (part c)) and two minima (a relative minimum (part d) and an absolute one (part e)) of this more complex pulsating behavior (part a of the same figure). Many similarities can be found between the features of Figure 9 and Figure 10, but, parts d and e of Figure 10 clearly show that at its minima the reaction proceeds without melting of zirconium. Both the temperature and ($\partial\eta/\partial t$) profiles clearly indicate that zirconium melting point is reached only in the so-called after-burn zone, behind the front, when the oxidation has been completed. This dilution degree is actually a limiting case: further dilution leads in fact to the extinction of the process.

When the $P(O_2)$ is as low as to control the reaction mechanism, the stationary propagation mode directly turns into extinction. Figure 11 shows the trend of combustion temperature and wave velocity as a function of dilution degree at $P(O_2) = 10^{-3}$ atm, where pressure control is active. As dilution is increased the two models provide coincident values of both parameters. Interestingly, this occurs at temperatures above zirconium melting; this indicates that, when pressure control is active, zirconium melting does not affect the reaction characteristics, while melting of the product oxide determines the usual

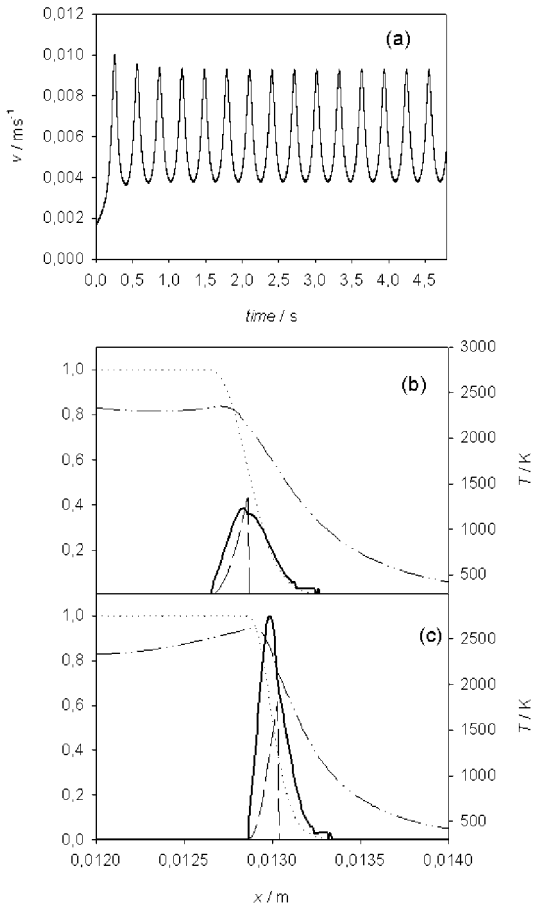

Figure 9. SHS at $P(O_2) = 1$ atm and $D = 0.85$ with phase transitions. Plot a: wave velocity as a function of time. Plots b and c: space profiles of temperature (dash−dot line, right axis), reaction rate (continuous line) and fraction of molten Zr (dashed line, left axis) at times corresponding to the maximum (plot c) and the minimum (plot b) of the wave speed.

noticeable difference in wave speed and combustion temperature at the low dilutions.

4. Conclusions

Before trying to generalize the insights of the above results, it is important to point out that only two phase transitions are here considered: the first one (melting of the reagent) occurs at a lower temperature than the second one (melting of the product). The enthalpy change of the first transition is significantly lower than that of the second one, and finally the combustion temperature never exceeds the transition temperature of the product (for all values of the process parameters that is reasonable to consider).

Moreover, no (explicit) kinetic law is assumed in the model for all phase transitions, which occur as far as "there is enough heat". The occurrence of a phase transition is expected to affect SHS propagation (a) by changing the enthalpy of a chemical reaction, (b) by its indirect effect on thermal conduction, and (c) by directly controlling the rate of some heat release process. In the present simulation, only the first two effects are included.

Concerning the first point, the most apparent effect is the significantly lowering of combustion temperature and wave speed. The former parameter, in particular, takes a well defined value (i.e., melting point of the product) which does not depend on process parameters in a wide range. As explained in the second section, from the point of view of a simple comparison between the simulations with and without phase transition, the

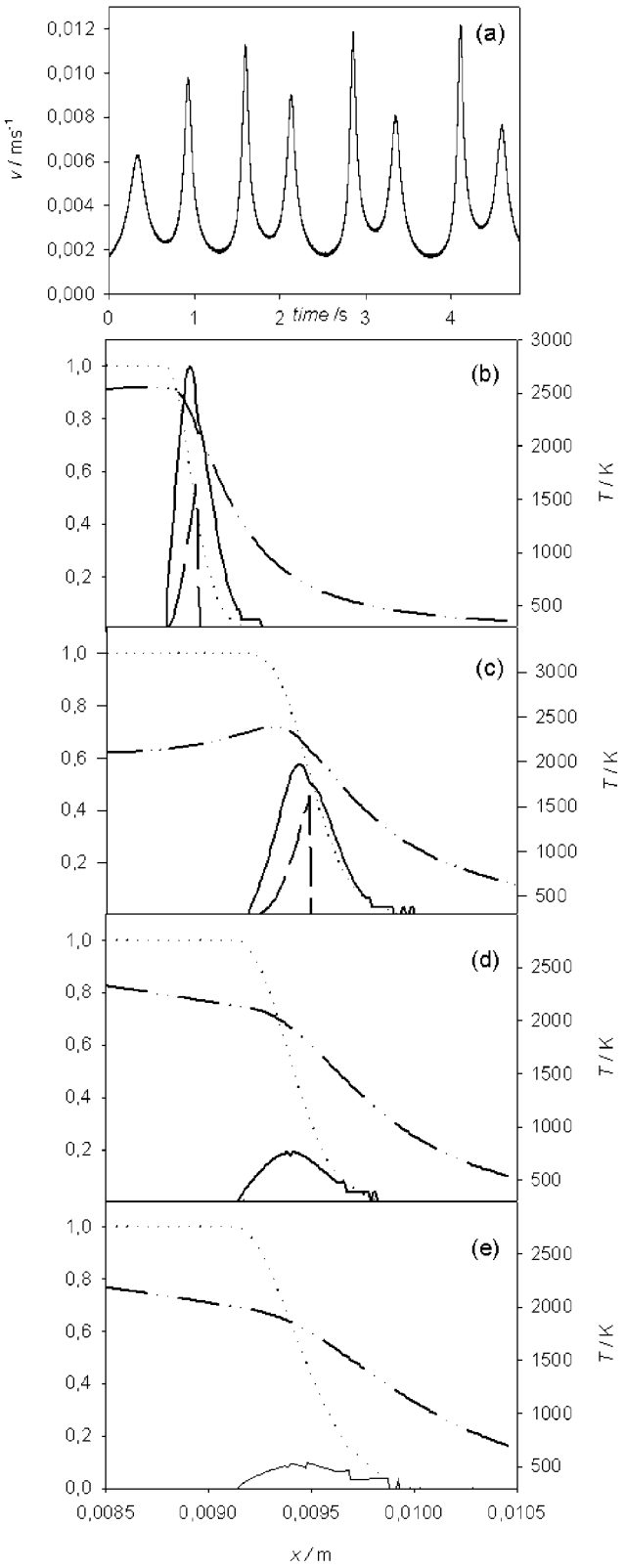

Figure 10. SHS at $P(O_2) = 1$ atm and $D = 0.86$. Plot a: wave velocity as a function of time. Plots b−e: space profiles of temperature (dash−dot line, left axis), reaction rate (continuous line,right axis), fraction of molten Zr (dashed line, right axis), and conversion degree of the oxidation (dotted line, right axis) at times corresponding to the absolute maximum (plot b), the relative maximum (plot c), the relative minimum (plot d), and the absolute minimum (plot e) of the wave speed.

observed difference is largely due to the significant reduction of the adiabatic temperature of the SHS reaction when melting of zirconia is added (an additional cause is discussed below).

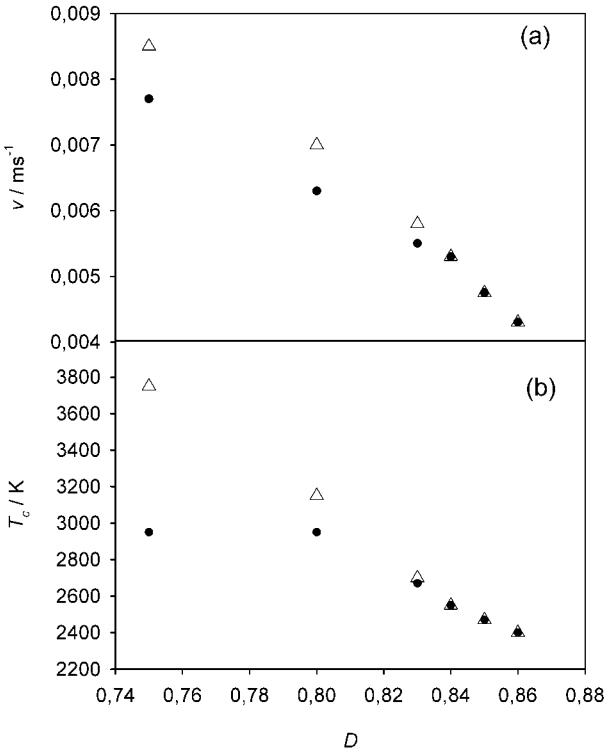

Figure 11. Combustion temperature (T_c, plot b) and wave speed (plot a) as a function of D at $P(O_2) = 10^{-3}$ atm with (full circles) and without (empty triangles) phase transitions. With $D \leq 0.8$ melting of zirconia occurs, melting of Zr occurs for all cases. Using the model without phase transitions, the combustion is stationary up to $D = 0.85$, with phase transition (that is, with Zr melting) the combustion is stationary up to $D = 0.86$.

Nonetheless, this difference provides a useful insight on mechanisms of an SHS process. This effect holds as long as the combustion temperature reaches the melting point of zirconia. Moreover, when progressively more exothermic conditions are considered, a larger amount of zirconia (product or diluent) melts, and an increasing lowering of macro-kinetics (with respect to the absence of phase transitions) is observed.

The above effect must be expected for all phase transitions concerning a reaction product or a diluent (or else a reagent, as far as it is present in the starting mixture in excess of stoichiometry). On the contrary, any transition enthalpy concerning a reagent (or, more precisely, the part of a reagent that is completely consumed by the SHS process) does not change the overall energy balance and therefore is "neutral" to a first approximation.

However, the presence of any kind of phase transition also markedly affects the heat transport and heat generation processes, and produces many other effects.

As a sort of second order effect, zirconium melting also produces a well clear enhancement of the reaction rate and a knee of the thermal profile when the local temperature crosses the transition temperature (see, for instance, Figure 5). In simple words, the effect can be explained by considering that zirconium melting increases the reaction enthalpy (which increases the rate of heat release and consequently the rate of heat propagation into the region where the transition is already complete). Hopefully, this effect can be observed in the experimental determination of temperature profiles, and therefore can be used for the interpretation of SHS experiments, where it can possibly appear in an enhanced manner by a possible enhancement of oxidation rate of the molten reagent (not accounted for by our

simulations). Ahead of the melting front, on the contrary, heat propagation is decreased by the marked effect of the transition enthalpy (with respect to the effect of heat capacities alone) on energy uptake and on the temperature gradient.

Finally, a very important general effect of phase transitions can be referred to as a "damping" or "stabilizing" effect. The region of process parameters space corresponding to steady propagation is significantly enlarged by inserting the phase transitions, although the propagation parameters are lower. The propagation appears as more "close to steady behavior" also after the onset of pulsating modes, as shown by the smaller difference between oscillation minima and maxima and by the displacement of the limits of the extinction region. Another related feature is the shortening of the initial transient due to ignition in the parameter region pertinent to steady combustion. In all cases, this effect has to be related to the phase transition of the zirconium reagent and is pertinent to the cases where the combustion process is fully controlled by solid-state diffusion.

As a general comment, we note that the addition of the phase transitions produces many different effects that can be a priori predicted only in few cases. The computer simulation gives a full information on the complex process occurring in an SHS in form of space and time profiles of the whole set of variables (temperature and advancement degrees) and therefore makes possible to gain a complete understanding of the underlying mechanisms, which is usually impossible with real experiments, where a more limited information is typically available. Moreover, the phase transitions produce, in some cases, well defined features also on the directly measurable quantities, and on their dependence on process variables: then their presence in a real experiment can be used as a useful insight of the relevance of a phase transition in an SHS mechanism.

References and Notes

(1) Merzhanov, A. G.; Boroviskaya, I. P. *Dokl. Acad. Sci. USSR (Chem.)* **1972**, *204*, 429.
(2) Merzhanov, A. G. *Comb. Sci. Technol.* **1994**, *98*, 307.
(3) Moore, J. J.; Feng, H. J. *Prog. Mater. Sci.* **1995**, *39*, 243.
(4) Moore, J. J.; Feng, H. J. *Prog. Mater. Sci.* **1995**, *39*, 275.
(5) Munir, Z. A. *Am. Ceram. Soc. Bull.* **1988**, *67*, 342.
(6) Munir, Z. A.; Anselmi-Tamburini, U. *Mater. Sci. Rep.* **1989**, *3*, 277.
(7) Varma, A.; Lebrat, J.-P. *Chem. Eng. Sci.* **1992**, *47*, 2179.
(8) Mercer, G. N.; Weber, R. O. *Proc. R. Soc. London A* **1995**, *450*, 193.
(9) Weber, R. O.; Mercer, G. N.; Sidhu, H. S.; Gray, B. F. *Proc. R. Soc. London A* **1997**, *453*, 1105.
(10) Bayliss, A.; Matkowsky, B. J. *SIAM J. Appl. Math.* **1990**, *50*, 437.
(11) Bayliss, A.; Matkowsky, B. J. *SIAM J. Appl. Math.* **1994**, *54*, 147.
(12) Matkowsky, B. J.; Sivashinsky, G. I. *SIAM J. Appl. Math.* **1978**, *33*, 465.
(13) Arimondi, M.; Anselmi-Tamburini, U.; Gobetti, A.; Munir, Z. A.; Spinolo, G. *J. Phys. Chem. B* **1997**, *101*, 8059.
(14) Maglia, F.; Anselmi-Tamburini, U.; Gennari, S.; Spinolo, G. *Phys. Chem. Chem. Phys.* **2001**, *3*, 489.
(15) Makino, A. *Prog. Energ. Combust.* **2001**, *27*, 1.
(16) Weast, R. C., Ed. *Handbook of Chemistry and Physics*, 67th ed.; The Chemical Rubber Co.: Boca Raton, FL, 1986−1987.
(17) Anselmi-Tamburini, U.; Spinolo, G.; Munir, Z. A. *J. Mater. Synth. Process* **1993**, *1*, 323.
(18) Anselmi-Tamburini, U.; Arimondi, M.; Maglia, F.; Spinolo, G. *J. Am. Ceram. Soc.* **1998**, *81*, 1765.